

Optimising Sisal Fibre-Reinforced Self-Compacting Mortar blended with Glass Powder for improved Mechanical Properties



M. A. Akinpelu, W. A. Ajibowu*, A. M. Salman, A. G. Abdullah, A. B. Olahan

Department of Civil engineering, Kwara state University, Malete, Kwara state, Nigeria



ABSTRACT: Sustainable alternatives are needed to reduce cement consumption while maintaining self-compacting behavior and enhancing toughness, ductility, and durability. Sisal fiber, with its high tensile strength and crack-bridging ability, improves ductility, while recycled glass powder (GP), due to its pozzolanic properties, reduces cement use and densifies the matrix. However, their combined effects in self-compacting mortar (SCM) remain underexplored. In this study, a Central Composite Design (CCD), implemented within a Design of Experiments (DoE) framework using Design-Expert software, was employed to statistically model and optimize the effects of GP and sisal fiber. GP replaced cement at 0–22.5%, while sisal fiber (SF) was incorporated at 0–1% by volume. Binder content, sand (14.3 kg), and water (4948 ml) were kept constant. Specimens (50 mm cubes and 40 × 40 × 160 mm beams) were vibrated, cured at room temperature for 24 hours, submerged in water at ~27 °C, and tested at 7, 28, 56, and 90 days. Results show that SF enhances compressive and flexural strength, especially when combined with GP. Microstructural analysis revealed an increased amorphous hydration matrix associated with GP incorporation and suggested enhanced pozzolanic-related phases in SF-modified mixes. The optimal mix (7.5% GP, 0.5% SF) achieved a balance of strength, supporting its potential use in eco-friendly construction.

KEYWORDS: Industrial waste materials, Mechanical properties, Microstructure, Self-compacting mortar, Sustainable construction.

[Received Aug. 16, 2025; Revised Dec. 14, 2025; Accepted Jan. 02, 2026]

Print ISSN: 0189-9546 | Online ISSN: 2437-2110

I. INTRODUCTION

Self-compacting mortar (SCM) is a highly flowable, non-segregating mortar that spreads into place and fills formwork without the need for mechanical compaction (Nécira & Abadou, 2021). This type of mortar has properties similar to self-compacting concrete (SCC) but is used in applications where a more refined mixture is required, such as for smaller sections, repairs, or when precise filling of voids is necessary. The construction industry has become a major focus of research, especially in concrete technology. The increasing demand for infrastructure in urban areas has led to heightened development activities worldwide, significantly boosting the demand for concrete (Adesina & Awoyera, 2019). However, this demand poses a substantial environmental threat due to the high levels of greenhouse gas emissions—particularly carbon dioxide—associated with the production of Ordinary Portland Cement, which is the most carbon-intensive component of concrete. To address this, incorporating industrial waste materials into construction has gained considerable attention as a means to develop greener and more sustainable building materials. Recycling glass waste can help mitigate some issues associated with glass manufacturing, but the process is not entirely sustainable or cost-effective. Using glass powder in concrete manufacturing presents several challenges, including maintaining uniform particle size distribution, ensuring consistent quality and purity from recycled sources, and developing optimal mix designs through rigorous testing (Hassani et al., 2023). Long-term durability

assessment, especially under harsh conditions, is crucial, as concrete faces multiple simultaneous effects that have not been fully tested in real-world environments. To tackle these challenges, various recycling methods have been adopted over the past decade to reuse waste glass, and its potential applications in the construction industry, particularly in concrete, are being actively researched (Olofinnade et al., 2017).

Sisal fiber, a natural reinforcement derived from the *Agave sisalana* plant, has garnered attention for its potential to improve the mechanical properties of cement-based materials. Its high tensile strength, lightweight nature, and biodegradability make sisal fiber an attractive alternative to synthetic reinforcements (More & Subramanian, 2022). When integrated into self-compacting mortar (SCM), sisal fiber can enhance ductility, tensile strength, and energy absorption, thereby contributing to the overall performance of the material (Rafi et al., 2025). However, the biodegradability of sisal fibers also raises durability concerns, particularly in the highly alkaline environment of cementitious matrices. Exposure to calcium hydroxide and moisture can lead to fiber degradation through alkali attack, mineralization, and loss of interfacial integrity, resulting in reduced fiber tensile capacity and a gradual decline in crack-bridging effectiveness over time (Lv & Liu, 2023; Wei & Meyer, 2015). This degradation may adversely affect long-term durability indicators such as resistance to cracking, permeability, and dimensional stability. Nevertheless, several studies report that appropriate fiber

*Corresponding author: ajibowuwasiu123@gmail.com

treatment (alkali, silane, or pozzolan-rich matrices) and controlled fiber dosage can mitigate degradation by improving fiber–matrix bonding and reducing pore solution alkalinity, thereby enhancing the durability performance of sisal-reinforced mortar systems (Rodier & Savastano, 2018; Sales et al., 2015). Various studies have been conducted on sustainable materials in Self compacting mortar. Hammat et al. (2021) investigated the effect of natural pozzolana (NP) on the rheological, strength, shrinkage, and water absorption properties of self-compacting mortar.

Results showed that higher NP content and fineness reduced flowability but improved long-term strength. Increased NP fineness enhanced strength but increased both total and autogenous shrinkage. Higher NP content increased water absorption, while finer NP slightly reduced it. Horsakulthai (2021) examined the chemical composition of recycled concrete powder (RCP) and its effect on the physical properties of self-compacting mortar (SCM) when used as a supplementary cementitious material. RCP, sourced from crushed concrete, replaced ordinary Portland cement at 20%, 40%, and 60% by weight. Compressive strength, electrical resistivity, porosity, and water absorption were measured. Results showed RCP had a strength-activity index of 89.4% (7 days) and 87.2% (28 days). Increasing RCP content raised porosity and water absorption while reducing resistivity. The optimal RCP replacement for minimal strength loss was 20%.

Bentlemsan et al. (2023) explored the use of marble waste fine particles (MW) as a replacement for natural sand in self-compacting mortar (SCM). Substitution levels of 0%, 15%, 30%, 75%, and 100% were tested to evaluate their effects on fresh and hardened properties, as well as sulfate durability. Results indicate that up to 50% sand replacement maintains good workability and flow time. At 30% and 50% replacement, compressive and flexural strengths increase by 90 days, while porosity decreases at 30%. Mortars with up to 50% MW replacement also showed improved resistance to sulfate attack after 180 days. SEM and EDX analyses detected no significant ettringite formation. Sara et al. (2023) investigated the use of recycled concrete sand (RCS) as a substitute for natural sand and ground granulated blast furnace slag (GGBFS) as a cement replacement in self-compacting mortar (SCM) production. Fifteen mortar mixes were formulated with 0%, 25%, 50%, 75%, and 100% RCS replacing natural sand, and 0%, 20%, and 40% GGBFS replacing cement. The results show that SCM can be effectively produced with up to 50% RCS. Although RCS increases porosity and water absorption, these effects can be mitigated by using GGBFS. A 20% GGBFS replacement also improves long-term compressive strength. Souza et al. (2023) investigated the use of Superabsorbent Polymers (SAP) in self-compacting mortar (SCM) to control shrinkage and analyze thermal and mechanical properties, aiming for optimal

material proportions for large-volume structures. SCM mixes with 0%, 0.1%, and 0.2% SAP were tested with CII-E-32 and CPV-ARI cement under dry and submerged curing. Results showed SAP reduced temperature variation, suggesting its potential to mitigate thermal spikes in large structures. However, compression and tensile strengths decreased, except for tensile strength in CII-E-32, where SAP improved performance.

Optimization involves finding the action that best achieves a desired goal or objective, typically by maximizing or minimizing the value of an objective function (Maraghechi et al., 2014). The concept of optimization plays a significant role in human affairs as it embodies the drive to achieve the most favorable outcome in any given situation. Various optimization techniques exist, including linear programming, multi-local programming, convex programming, interactive optimization, genetic algorithms, and response surface methodology (Byrne, 2014). This research investigates the impact of sisal fiber reinforcement and glass powder on self-compacting mortar's mechanical properties. It aims to determine the optimal proportions of sisal fiber and glass powder to enhance mortar performance while promoting sustainability. The study aims to evaluate the properties of self-compacting mortar with glass powder, assess its mechanical properties, analyze microstructural changes, and optimize the mix proportions for optimal performance, and sustainability. Recycling glass into powder form reduces cement use, CO₂ emissions, and waste management, while offering financial advantages like lower costs and improved performance.

II. MATERIALS AND METHODS

A. Materials

The materials used in a research project, including Portland Limestone cement, fine aggregate, water, and waste glass. The cement was purchased from Mohadis construction Limited in Ilorin, Kwara state, and the fine aggregate was obtained from Asa River in Ilorin. The water used in the mix was potable and conformed to BS EN 1008:2002. The waste glass was sourced from restaurants and processed into powder in Ladoke Akintola University of Technology, Ogbomosho, Ogbomosho. The glass was then mechanically crushed, ground to a particle size of 120 microns, and sieved through a 90-micron mesh to achieve a consistent particle size, used in study by Akinpelu et al. (2025). The sisal fibers were sourced from agricultural processing facilities in Ilorin, Kwara State, Nigeria, for their high tensile strength, durability, and resistance to moisture. The fibers underwent cleaning, sun-drying, and cutting to uniform lengths to ensure consistent dispersion and bonding within the mortar matrix. Sika superplasticizer was used to enhance the workability of the self-compacting mortar.



Figure 1 Glass powder



Figure 2 Sisal fiber

B. Mix Proportion and Experimental Set-up

The mix design in this study was structured to systematically investigate the combined effects of mortar replacement and sisal fiber content on mortar properties, using the Central Composite Design (CCD) in Design Expert software. Across all 12 mixes (M1–M12), the total binder content was maintained constant, while varying proportions of GP replaced ordinary Portland cement at levels of 0%, 7.5%, 15%, and 22.5%. Correspondingly, as GP content increased, the cement content decreased proportionally to ensure uniform binder

mass throughout. Sisal fiber content was also varied by volume across three levels: 0%, 0.5%, and 1%. The mix ratio used was 1: 2.75 with water-cement ratio of 0.5. While cement and GP quantities changed based on the designed replacement ratios, the sand quantity (14.3 kg) and water volume (4948 ml) remained constant for all mixes, allowing the study to isolate and assess the specific influence of GP and fiber content. This deliberate variation created a balanced and statistically sound matrix suitable for response surface analysis, enabling the prediction and optimization of mortar performance based on glass powder and natural fiber incorporation.

Table 1 The Mix proportion

Mix ID	GP Replacement (%)	Sisal Fiber Content (% Volume)	Sisal Fiber byContent (% by Volume)	Cement (kg)	GP (kg)	Sand (kg)	Water (ml)
M1	0	0	0	5.2	0	14.3	4948
M2	0	0.5	0.0104	5.2	0	14.3	4948
M3	0	1	0.052	5.200	0	14.3	4948
M4	7.5	0	0	4.810	0.39	14.3	4948
M5	7.5	0.5	0.0104	4.810	0.39	14.3	4948
M6	7.5	1	0.052	4.810	0.39	14.3	4948
M7	15	0	0	4.42	0.78	14.3	4948
M8	15	0.5	0.0104	4.420	0.78	14.3	4948
M9	15	1	0.052	4.420	0.78	14.3	4948
M10	22.5	0	0	4.03	1.17	14.3	4948
M11	22.5	0.5	0.0104	4.03	1.17	14.3	4948
M12	22.5	1	0.052	4.03	1.17	14.3	4948

To evaluate the mechanical properties of the mortar, three cube specimens with dimensions of $50 \times 50 \times 50$ mm, prepared

in accordance with BS EN 196-1 (2016), were used for compressive strength testing, while three prismatic beams

measuring $40 \times 40 \times 160$ mm, also conforming to BS EN 12390-5 (2009), were cast for flexural strength assessment, as shown in Figure 3.3. All specimens were compacted using a mechanical vibration table to ensure proper consolidation. After casting, they were left at ambient room temperature for 24 hours, demolded, and subsequently cured in water at approximately 27°C for 7, 28, 56, and 90 days prior to testing. Finally, statistical analysis was applied using tools such as Design-Expert software with Response Surface Methodology (RSM) to optimize the mix by minimizing the number of experimental trials and evaluating the effects of multiple variables, including glass powder content and fiber dosage, on strength development. Regression analysis was also employed to develop predictive models for strength based on the experimental data. The optimized mix design was subsequently validated by replicating the experiments and comparing the measured results with the predicted outcomes from the regression models, thereby ensuring that the desired mechanical properties of the SCC mortars were consistently achieved across different trials.

C. Chemical properties of glass powder

The chemical composition of the processed waste glass powder was analyzed using X-ray Fluorescence (XRF) spectrometry at the Integrated Research Laboratories in Ibadan, Oyo State. This method was employed to detect and quantify the elemental oxides within the material, providing critical information for assessing its potential as a supplementary cementitious material. The test followed the standard of ASTM E1621(2013). SEM was used to examine the surface morphology and internal structure of mortar after 7 days containing sisal fiber and glass powder. Samples were cleaned, dried, and cut to size before being mounted on conductive stubs and coated with gold or carbon. Imaging was conducted under vacuum at varying magnifications, and Energy Dispersive X-ray Spectroscopy (EDS) was used for elemental composition analysis. Observations focused on fiber-matrix bonding, pore distribution, and morphological changes. The analysis followed ASTM E1508 (2012) and was carried out at Integrated Research Laboratories, Ibadan. XRD was performed to identify crystalline phases in the mortar mixes after 7 days. Powdered samples were pelletized and sieved to 0.074mm . These were later taken in an aluminum alloy grid ($35\text{mm} \times 50\text{mm}$) on a flat glass plate and covered with a paper. Wearing hand gloves, the samples were compacted by gently pressing them with the hand. Each sample was run through the Rigaku D/Max-IIIc X-ray diffractometer developed by the Rigaku Int. Corp. Tokyo, Japan and set to produce diffractions at scanning rate of $2^\circ/\text{min}$ in the 2θ range of 2° – 50° at room temperature with $\text{CuK}\alpha$ radiation operated at 40 kV and 20 mA. The diffraction data (d value and relative intensity) obtained was compared to that of the standard data of minerals from the mineral powder diffraction file, ICDD which contained and includes the

standard data of more than 3000 minerals. Similar diffraction data means the same minerals to standard minerals which exist in the soil sample. Tests followed ASTM C1365-18. It was carried out at Integrated Research Laboratories, Ibadan.

D. Mechanical properties testing

Mechanical testing was carried out after curing, with compressive strength measured at 7, 28, 56, and 90 days. Flexural strength was also determined to evaluate the flexural performance of the mixes in accordance with BS EN 1015-11, while compressive strength testing was conducted following the same standard.

1) Compressive strength test

Mechanical testing was carried out after curing, with compressive strength measured at 7, 28, 56, and 90 days. Flexural strength was also determined to evaluate the flexural performance of the mixes in accordance with BS EN 1015-11, while compressive strength testing was conducted following the same standard. The compressive strength test was conducted to evaluate the load-bearing capacity of mortar mixes containing sisal fiber and waste glass powder. The materials were thoroughly mixed and cast into standard cube molds, cured for 7, 28, 56, and 90 days. Following each curing period, the samples were taken out of the curing tank, surface-dried, and tested using a Universal Testing Machine (UTM) at the University of Ilorin (Figure 3). Load was applied steadily until failure occurred, and the peak load sustained by each specimen was recorded. The test procedure conformed to BS EN 1015-11: 2019 standards, ensuring accuracy and consistency in evaluating the performance of the modified mortar mixes.



Figure 3 Compressive strength test

2) Flexural strength test

Flexural strength testing was conducted to assess the bending resistance of mortar mixes incorporating sisal fiber and waste glass powder (Figure 4). Prismatic specimens measuring $40 \times 40 \times 160$ mm were prepared and cured under standard laboratory conditions for 28 days. The test followed the procedures outlined in BS EN 1015-11:2019, which prescribes

methods for determining the flexural strength of hardened mortar. A three-point loading configuration was employed, where each prism was placed on two support rollers and subjected to a central load using a universal testing machine. The applied load was gradually increased until the specimen fractured, and the maximum load at failure was recorded.



Figure 4 Flexural strength testing

III. RESULT AND DISCUSSION

A. Characterization of glass powder

The XRF results (Table 2) confirm the pozzolanic potential of the glass powder used. SiO₂ content was 52.54%, while the

combined oxides (SiO₂ + Al₂O₃ + Fe₂O₃) amounted to 85.04%, surpassing the ASTM C618 minimum requirement of 70% for Class N pozzolans. These values indicate the material's suitability as a supplementary cementitious material.

Table 2: Chemical composition of glass Powder

Component	Content (wt.%)
SiO ₂	52.54
Al ₂ O ₃	28.85
Fe ₂ O ₃	3.65
MnO	0.01
CaO	1.94
P ₂ O ₅	-
K ₂ O	0.95
TiO ₂	1.17
MgO	0.08
Na ₂ O	0.05
LOI	10.2
Total (SiO₂ + Al₂O₃ + Fe₂O₃)	85.04

The XRD pattern in Figure 5 reveals sharp diffraction peaks corresponding to crystalline phases such as kaolinite, quartz, albite, and muscovite. The lack of a broad amorphous hump indicates that the material is predominantly crystalline,

suggesting a clay-derived or ceramic origin rather than soda-lime glass. This contrasts with the findings of (2025), who reported that their waste glass powder existed predominantly in an amorphous state.

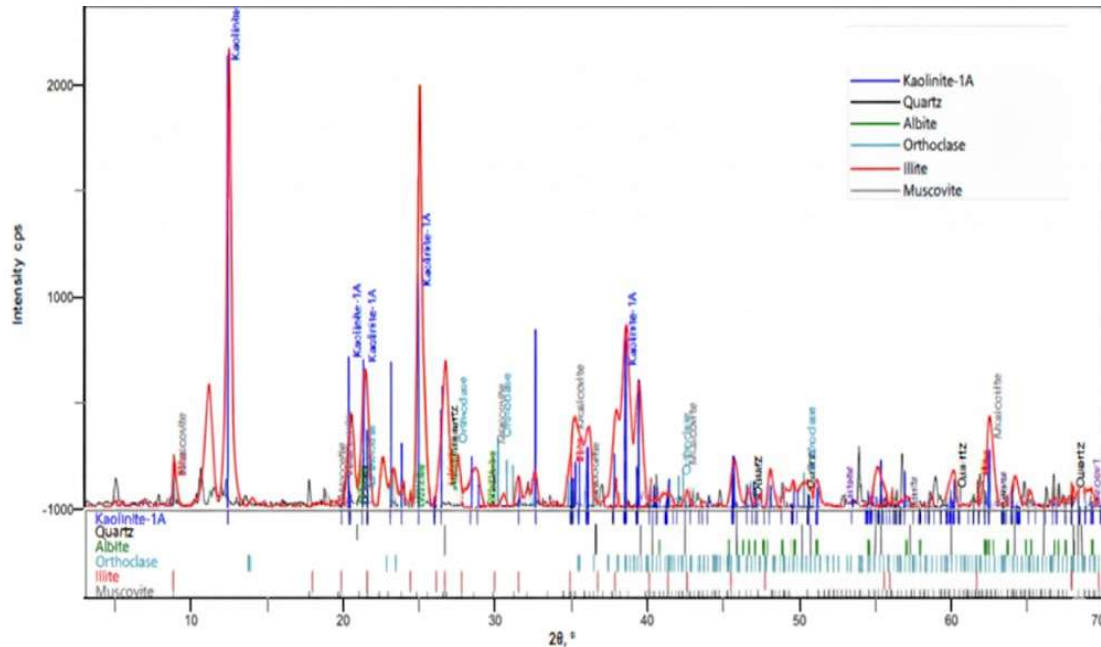


Figure 4 XRD pattern of glass powder

The scanning electron microscopy (SEM) image of the glass powder, illustrated in Figure 6 at a magnification of 10,000 \times and an accelerating voltage of 15 kV, displays a highly textured and uneven surface morphology. The particles exhibit jagged contours, layered formations, and notable internal voids. The appearance of sheet-like and plate-shaped elements implies the existence of thermally processed clay-based minerals—such as kaolinite or illite—which are commonly associated with calcined pozzolanic substances (Asonibare et al., 2025). These microstructural traits contribute to an expansive surface area, enhancing the material's reactivity with calcium hydroxide to form additional calcium silicate hydrate (C–S–H) during the cement hydration process. The irregular shape and porous composition of the particles also support improved matrix compaction and enhanced long-term performance in cement-based applications. However, such characteristics can elevate the water requirement, necessitating careful adjustment of the mix proportions or the use of water-reducing agents. This finding is consistent with the observations of Rath et al. (2025) along with Du & Tan (2014) who reported that the particles possess irregular morphologies, rough surface textures, and relatively high surface areas.

Figure 7 show the XRD pattern of samples. The M1 diffractogram (2θ 20–70°; peak width $\approx 0.065^\circ$) is dominated by sharp quartz reflections ($\approx 21^\circ$, 26.5° , 31° , 36° , 50°) with subordinate kaolinite, mica/illite-smectite and Fe-oxides, and a broad 20–25° hump consistent with amorphous C–S–H from partial hydration, indicating a typical cementitious mix of

crystalline silicates and amorphous hydration products. The result aligns with finding with Li & Scrivener (2025). M2 (0.5% sisal) pattern (2θ 5–75°) retains a highly crystalline quartz matrix ($\approx 21^\circ$, 27° , 31° , 39° , 50°) with kaolinite/mica and Ca/Fe oxides present; a low-angle amorphous hump and the appearance of weak zeolitic reflections suggest minor pozzolanic/secondary phases introduced or promoted by fiber treatment, while the main crystalline framework remains intact. This outcome aligned with research conducted by Fode et al. (2025). The M3 pattern (2θ 20–70°) shows the same quartz-dominated profile with preserved kaolinite and zeolite signatures, slightly reduced minor-phase intensities and a weak calcite peak ($\sim 48^\circ$), implying better matrix homogeneity and subtle microstructural changes (improved internal curing and refinement) with 1% fiber, as with findings of Lyu et al. (2025). In M4 (7.5% glass powder), the diffraction of the 7.5% glass mix is strongly quartz-dominated (notably $\approx 26.6^\circ$, 36.5° , 50°) with minor kaolinite, mica, Ca and Fe oxides and nascent zeolitic peaks; because glass itself is largely XRD-amorphous, its effect is inferred from increased amorphous C–S–H and secondary zeolitic products consistent with ongoing pozzolanic reactions (Li et al., 2022). In M5 (Figure 11, 15% glass powder), the 15% glass replacement the pattern remains quartz-rich but shows enhanced zeolitic and amorphous phase development and residual Ca-oxide reflections, indicating intensified pozzolanic transformation and greater amorphous C–S–H/zeolite formation at higher glass contents while preserving the crystalline framework. This coincides with the research outcomes of Ren et al. (2025).

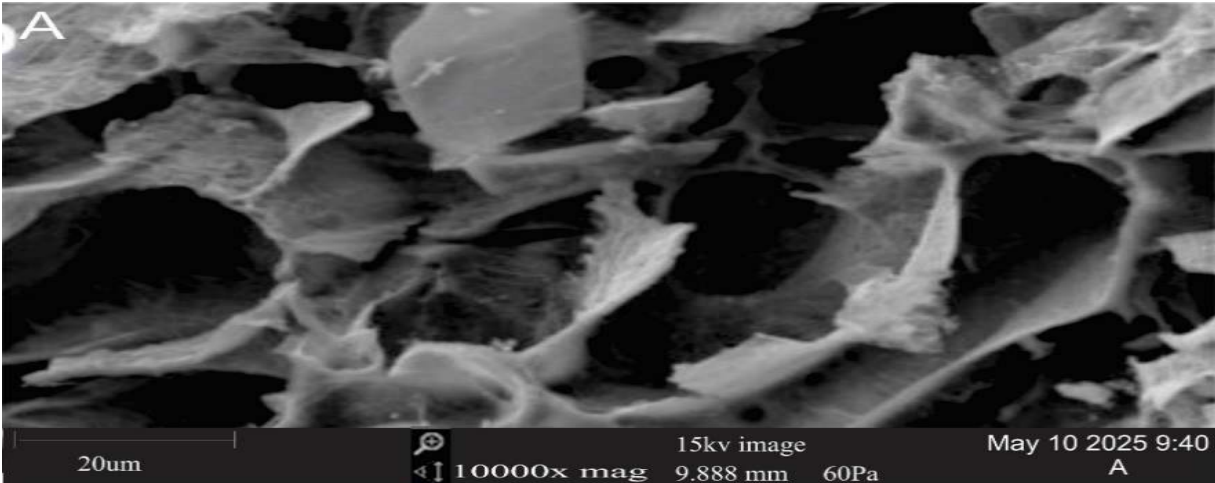


Figure 5 SEM image of Waste glass powder

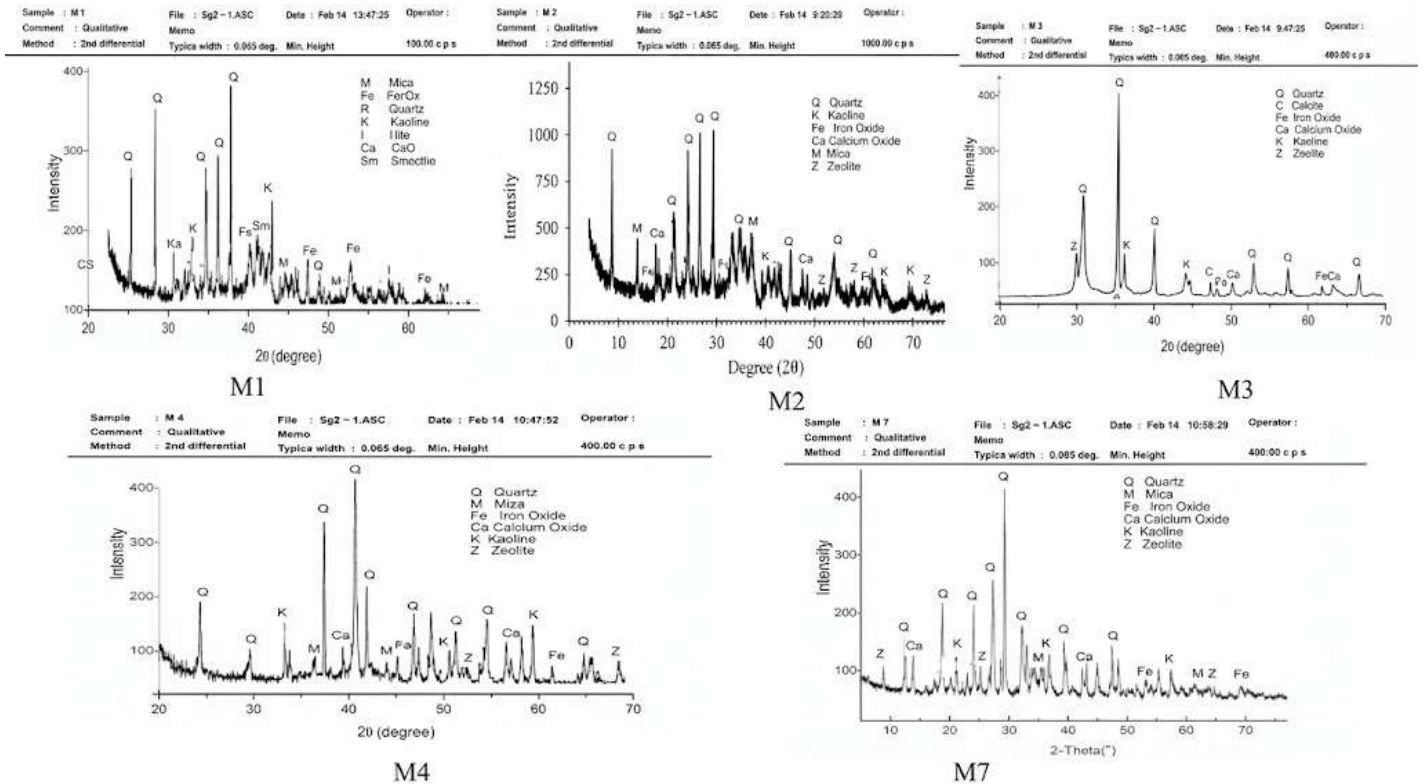


Figure 6 XRD pattern of samples

Figure 8 displays the SEM images of mortar samples. The High-magnification SEM of M1 shows an assembly of angular to sub-rounded particles with heterogeneous size distribution (fine to coarse), surface roughness, microfractures and interparticle pores consistent with brittle cementitious powders and partially hydrated surfaces; these features indicate a typical particle-packed matrix with open porosity that will govern early permeability and mechanical behavior (Ahmad et al., 2025). The micrograph of M2 reveals the

granular mortar matrix interspersed with elongated sisal fibrils that are variably bonded to the matrix (regions of intimate contact and partial debonding), highlighting interfacial pull-out and fiber-matrix adhesion phenomena that control toughness and post-crack behavior in natural-fiber composites (Qu et al., 2024). The SEM image of M3 displays a more heterogeneous, porous microstructure with numerous voids, microcracks and loosely bound particle clusters alongside spherical/sub-angular remnants of unhydrated grains; these

features suggest that 1% sisal increases matrix openness and disrupts local densification—effects that can reduce compressive stiffness but improve energy absorption and cracking resistance. The same findings was reported by Yimer & Gebre (2023). In M4 (7.5% glass powder), glass powder appears as smooth, rounded inclusions within an angular cement matrix, producing clear particle–matrix interfaces; the juxtaposition of glass (largely XRD-amorphous at this scale) and hydrated phases implies a combined filler and pozzolanic

action that improves packing while promoting amorphous C–S–H formation at the rims, same result found by Zhou et al. (2025). In M7 (15% glass powder), high additive content produces distinct, uniformly distributed secondary phases and well-defined interfacial zones—some showing strong bonding or reaction rims—indicating effective stress transfer and active pozzolanic/secondary phase development that substantially modifies pore structure and packing compared with the control. Same outcome reported by Akinpelu et al. (2025).

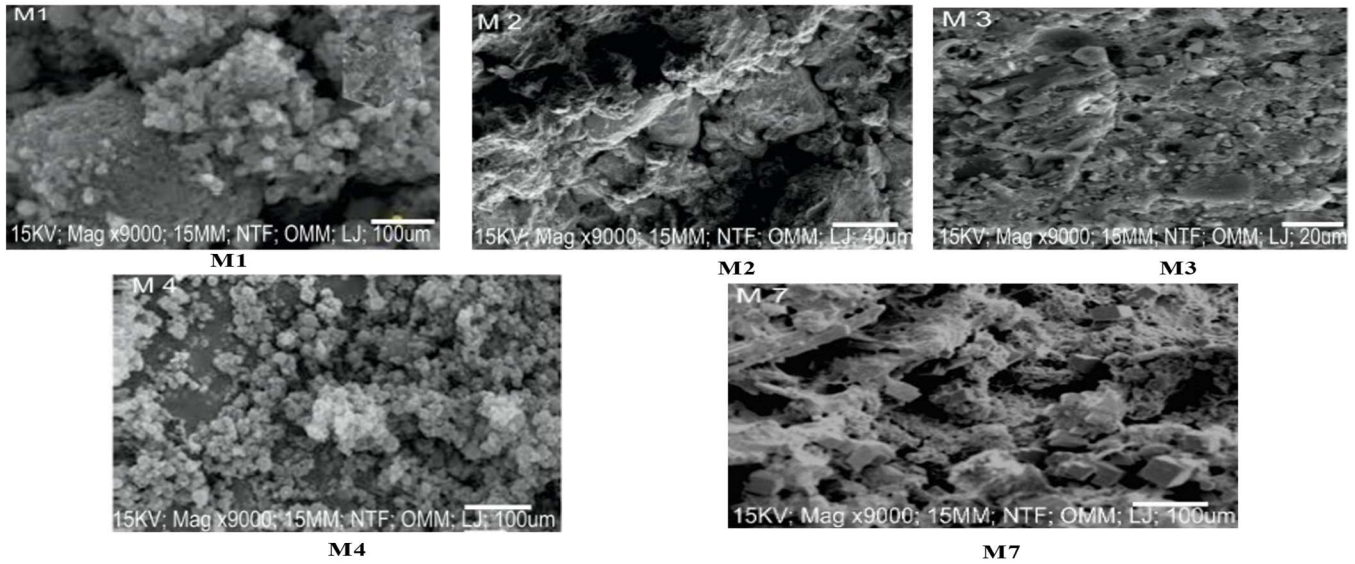


Figure 7 SEM images of samples

B. Compressive Strength Result

Compressive strength trends generally improved with curing age in all mixes, though the inclusion of ground waste glass powder (GWP) and fibers led to distinct variations. Mixes with high GWP replacement (22.5%), such as M11 and M12, exhibited relatively low early-age (7-day) strengths of 5.86–6.19 N/mm² but demonstrated the most aggressive strength gain by 90 days, reaching over 14–15 N/mm². This trend is characteristic of the slow pozzolanic reaction of glass powder, which contributes to later-age densification and strength development. The control mix (M1) achieved the highest

overall compressive strength at 90 days (17.501 N/mm²). However, M8 (15% GWP and 0.5% fiber) performed nearly as well, attaining 17.003 N/mm² at the same age, indicating that moderate GWP combined with fibers can yield comparable long-term performance to the reference mix. The addition of 0.5% fiber alone (M2) provided the highest 28-day strength across all mixes (17.247 N/mm²), suggesting that moderate fiber content effectively optimizes mid-term mechanical performance by enhancing crack resistance and load distribution. The compressive strength is shown in Table 3.

Table 3 Compressive strength results

Mix ID	Fiber (%)	GWP (%)	7 Days	28 Days	56 Days	90 Days
M1	0	0	9.131	14.895	15.526	17.501
M2	0.5	0	10.031	14.985	17.247	18.018
M3	1	0	12.549	16.001	17.856	19.039
M4	0	7.5	9.131	10.934	14.071	14.910
M5	0.5	7.5	9.947	11.998	14.522	16.577
M6	1	7.5	8.733	11.322	12.661	15.185

M7	0	15	8.500	10.120	13.560	14.093
M8	0.5	15	7.687	7.811	11.483	14.667
M9	1	15	8.724	9.670	10.670	13.679
M10	0	22.5	6.300	7.503	9.053	12.396
M11	0.5	22.5	5.86	5.939	6.372	11.982
M12	1	22.5	6.197	8.093	9.669	12.751

The 3D surface plot in Figure 9 illustrates the relationship between the 90 days compressive strength of mortar (in N/mm²) and the combined effects of waste glass and sisal fiber content. The compressive strength exhibits a linear trend with varying proportions of these two additives. As the powder replaces cement in the mortar, the compressive strength

decreases. In contrast, the addition of sisal fiber shows a consistent positive effect on compressive strength across increasing dosages. The fiber appears to enhance strength through mechanisms such as crack bridging and improved stress distribution within the matrix.

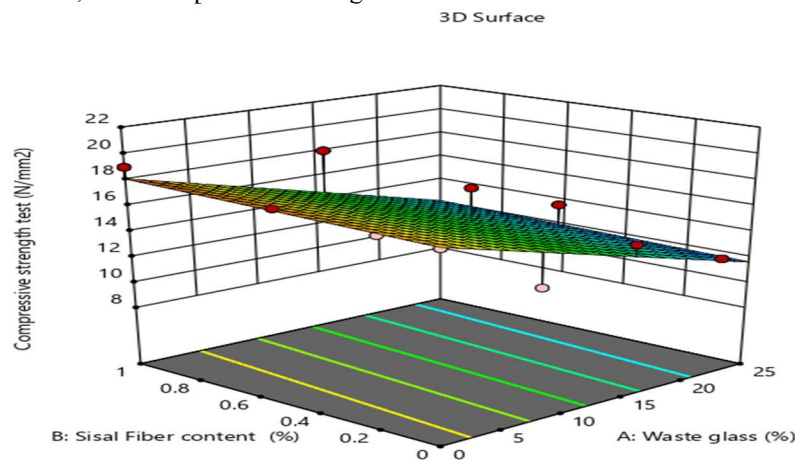


Figure 8 Compressive strength result

Flexural strength trends were generally more stable than compressive strength results, indicating that the mortar maintained good resilience under bending loads across all mixes and curing ages. The addition of 1% fiber in M3 (with 0% GWP) significantly enhanced flexural performance, achieving a high value of 7.221 N/mm² at 90 days. Notably, M7 (15% GWP and 0% fiber) exhibited the highest overall flexural strength at 90 days (7.223 N/mm²), suggesting that a 15% glass powder replacement level may represent an optimal for improving the internal microstructure and thereby maximizing flexural resistance without fibers. However, at the highest replacement level (22.5% GWP), flexural strength was consistently lower across all curing ages compared to mixes with 0% or 15% GWP, highlighting a limitation of excessive glass powder incorporation in terms of bending performance. Table 4 show the flexural strength of mortar mixes.

After 90 days of curing, the 3D relationship between flexural strength, sisal fiber content, and glass powder content reveals a synergistic effect on the mechanical performance of the mortar. The incorporation of sisal fiber contributed to enhanced flexural strength by bridging microcracks and improving the toughness and ductility of the composite, supporting the findings of Zhou et al. (2024). Simultaneously, the addition of glass powder, due to its pozzolanic reactivity, promoted additional cementitious reactions, leading to a denser microstructure and further strength gain like in the results of Maraghechi et al. (2014). Together, these materials worked to significantly improve the flexural behavior of the mortar, with both components playing complementary roles in strengthening the matrix. The result is displayed on Figure 10.

Table 4: Flexural Strength Result

Mix ID	Fiber (%)	GWP (%)	7 Days	28 Days	60 Days	90 Days
M1	0	0	4.831	6.125	6.337	5.493
M2	0.5	0	4.859	5.851	5.523	5.625
M3	1	0	5.279	6.985	6.59	7.221
M4	0	7.5	4.629	5.683	5.516	6.315
M5	0.5	7.5	4.787	6.441	6.187	6.238
M6	1	7.5	4.276	5.266	4.883	6.255
M7	0	15	4.676	6.792	5.597	7.223
M8	0.5	15	3.949	5.836	6.166	6.245
M9	1	15	3.885	5.234	5.677	6.225
M10	0	22.5	3.757	5.395	5.849	6.561
M11	0.5	22.5	2.835	4.408	5.213	6.188
M12	1	22.5	3.008	4.036	5.386	5.144

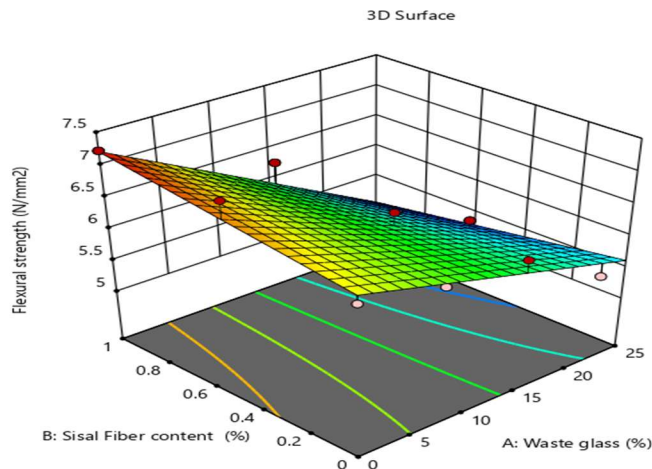


Figure 9 Flexural strength result

A linear regression model was developed to estimate the compressive strength (in N/mm²) of mortar based on waste glass (WG) and sisal fiber (SF) content. The final equation in terms of actual factor levels is given in Equation (1). A First-order regression model was formulated to predict the flexural strength (in N/mm²) of mortar as a function of waste glass (WG) and sisal fiber (SF) content. The final equation in terms of actual factor levels is as given in Equation (2).

$$\text{Compressive Strength} = 17.28 - 0.236 \cdot \text{WG} + 0.791 \cdot \text{SF} \quad (1)$$

$$\text{Flexural Strength} = 6.69 - 0.043 \cdot \text{WG} + 0.525 \cdot \text{SF} - 0.044 \cdot (\text{WG} \times \text{SF}) \quad (2)$$

Where, WG = Waste Glass (%) and SF = Sisal Fiber (%)

The ANOVA analysis confirms that both the compressive strength and flexural strength models are highly statistically significant ($P < 0.0001$), demonstrating that the experimental

factors—such as ground waste glass powder (GWP) replacement levels, fiber content, and their interactions—strongly influence the mechanical properties of the self-compacting mortar. The compressive strength model exhibits excellent fit and predictive capability, with a mean square of 26.54, F-value of 49.96, R^2 of 0.909 (explaining 90.9% of the variability), adjusted R^2 of 0.8908, predicted R^2 of 0.8454, and adequate precision of 17.441 (well above the recommended threshold of 4). In contrast, the flexural strength model is slightly less precise but still robust, with a mean square of 1.56, F-value of 25.7, R^2 of 0.8955 (explaining 89.6% of the variability), adjusted R^2 of 0.8606, predicted R^2 of 0.7856, and adequate precision of 14.3191. Overall, both models are statistically valid and reliable, with the compressive strength model showing marginally better explanatory power and precision, suggesting that compressive behavior is more

consistently influenced by the factors than flexural strength, which may be more sensitive to microstructural variations.

Figure 11 illustrates the optimized mortar mix design, revealing that the inclusion of approximately 7.5% waste glass and 0.5% sisal fiber significantly enhances mechanical performance. This composition achieves a flexural strength of

6.46 MPa and a compressive strength of 15.89 MPa, while attaining a perfect desirability score of 1.000 — signifying an optimal balance between structural efficiency and sustainability. The overarching objective is to identify a mix that maximizes mechanical strength while integrating environmentally friendly materials.

Table 5: validation of results

Property	Mean Square	F-Value	P-value	R ²	Adjusted R ²	Predicted R ²	Adeq Precision
Compressive Strength	26.54	49.96	< 0.0001	0.909	0.8908	0.8454	17.441
Flexural Strength	1.56	25.7	< 0.0001	0.8955	0.8606	0.7856	14.3191

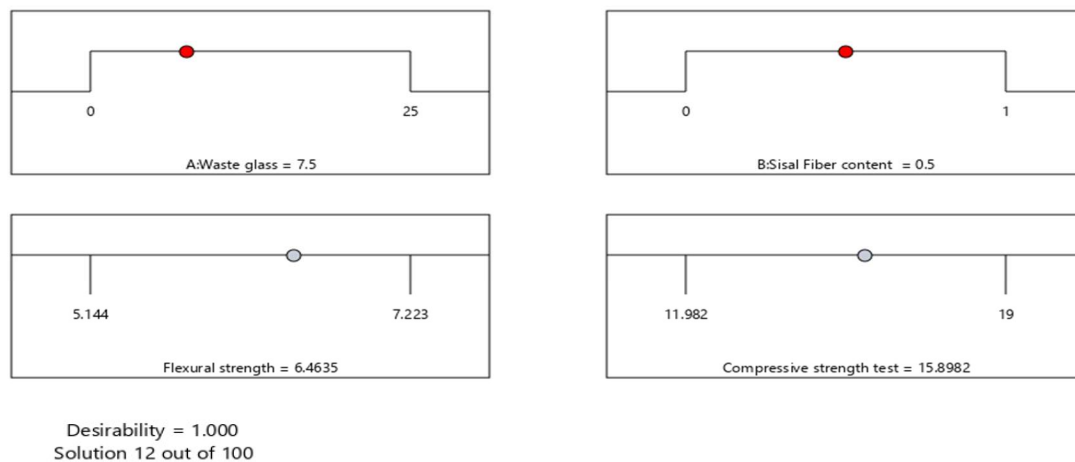


Figure 10 Optimized Results

IV. CONCLUSIONS

This study investigated the combined effects of waste glass powder (GP) as a partial cement replacement and sisal fiber (SF) reinforcement on the mechanical and microstructural properties of self-compacting mortar (SCM). The findings demonstrate that while higher GP replacement levels (up to 22.5%) reduce early-age compressive strength due to slower pozzolanic reactions and matrix dilution, the incorporation of sisal fiber consistently enhances both compressive and flexural performance through effective crack-bridging and improved stress distribution. The 90-day compressive strength of M3 (1% fiber, 0% GP) reached 19.04 N/mm², a 9% increase over the control, while M7 (15% GP, 0% fiber) achieved the highest flexural strength of 7.22 N/mm², indicating that optimal GP content alone can maximize bending resistance. Microstructural analyses via XRD and SEM revealed that GP contributes to a more continuous and densified hydration

matrix through increased formation of amorphous C–S–H from pozzolanic reactions, while sisal fibers exhibit mechanical interlocking within the cementitious matrix despite increased porosity at higher fiber contents. The appearance of zeolitic phases in SF-modified mixes further suggests enhanced pozzolanic activity associated with fiber incorporation. Statistical modeling using response surface methodology yielded highly significant predictive models for both compressive ($R^2 = 0.909$) and flexural strength ($R^2 = 0.896$), confirming the reliability of the experimental approach. Optimization analysis identified the ideal mix composition as 7.5% GP and 0.5% SF, achieving predicted strengths of 15.89 N/mm² (compressive) and 6.46 N/mm² (flexural) with a desirability score of 1.000. This optimal blend successfully balances structural efficiency with sustainability by reducing cement consumption and diverting glass waste from landfills while utilizing natural sisal fibers. The study

establishes that strategic combination of waste glass powder and sisal fiber offers a viable pathway for producing eco-friendly self-compacting mortar with enhanced mechanical properties, supporting the construction industry's transition toward more sustainable practices. Further research is recommended to evaluate long-term durability under aggressive environmental conditions.

AUTHOR CONTRIBUTIONS

Mutiu Adelodun Akinpelu led the research design, experimental planning, and final manuscript revision. **Wasiu Akanbi Ajibowu** conducted laboratory testing, data acquisition, and manuscript preparation. **Ash-Shu'ara Marafa Salman** coordinated materials selection, supervised mix development and revised the first draft. **Abdulwahab Gbenga Abdullah** performed data analysis and interpretation. **Abdulmajeed Bolaji Olanhan** supported validation, review, and refinement of the first draft. All authors reviewed and approved the final version of the paper.

REFERENCES

- Adesina, A., and P. Awoyera** (2019). Overview of trends in the application of waste materials in self-compacting concrete production. *SN Applied Sciences*, 1(9). <https://doi.org/10.1007/s42452-019-1012-4>
- Ahmad, J.; M. M. Sabri; A. Majdi; W. Alattyih; I. Khan; and M. Alam** (2025). Durability and microstructure aspects of sustainable concrete made with ceramic waste: A review. *Frontiers in Materials*, 11: 1508989. <https://doi.org/10.3389/FMATS.2024.1508989/BIBTEX>
- Akinpelu, M. A.; O. Amao; A.-S. M. Salman; and D. S. Gabriel** (2025). Sustainable self-compacting concrete: A study on the combined effects of waste glass powder and metakaolin as cement replacements. *Research on Engineering Structures & Materials*. <https://doi.org/10.17515/resm2025-610ma0105rs>
- Akinpelu, M. A.; A. A. Olayiwola; A.-S. M. Salman; M. R. Ibrahim; and Z. T. Giwa** (2025). Durability of sisal fiber-reinforced mortar with glass powder as cement substitute in aggressive environment. *Discover Concrete and Cement*, 1(1): 1–23. <https://doi.org/10.1007/S44416-025-00027-3>
- Asonibare, I.; R. Abdulwahab; and M. Adisa** (2025). Effect of pulverized burnt clay waste as a partial replacement of cement on the fresh and mechanical properties of concrete. *Discover Concrete and Cement*, 1(1): 1–15. <https://doi.org/10.1007/S44416-025-00016-6>
- ASTM Standard E1621** (2013). Standard guide for elemental analysis by wavelength dispersive X-Ray fluorescence spectrometry. American Society of Testing Materials.
- Bentlemsan, N.; W. Yahiaoui; and S. Kenai** (2023). Strength and durability of self-compacting mortar with waste marble as sand substitution. *Case Studies in Construction Materials*, 19. <https://doi.org/10.1016/j.cscm.2023.e02331>
- British Standards** (2009). BS EN 12390-5 - Flexural Strength of Test Specimens. British Standard Institutes, 37.
- British Standards Institution BSI** (2016). BSI 196-1:2016 Methods of testing cement Part 1: Determination of strength. British Standard.
- Byrne, C. L.** (2014). A first course in optimization. *A First Course in Optimization*. <https://doi.org/10.1201/b17264>
- de Souza, M. H. B.; L. R. R. Silva; V. A. dos S. Ribeiro; P. C. Gonçalves; M. de L. N. M. Melo; C. E. M. Gomes; and V. C. dos Santos** (2023). Influence of superabsorbent polymer in self-compacting mortar. *Buildings*, 13(7). <https://doi.org/10.3390/buildings13071640>
- Fode, T. A.; Y. A. C. Jande; Y. D. Kim; M. G. Ham; J. Lee; T. Kivevele; and N. Rahbar** (2025). Effects of different lengths and doses of raw and treated sisal fibers in the cement composite material. *Scientific Reports*, 15(1): 1603. <https://doi.org/10.1038/S41598-025-86046-3>
- Hamat, S.; B. Menadi; S. Kenai; C. Thomas; M. S. Kirgiz; and A. G. de Sousa Galdino** (2021). The effect of content and fineness of natural pozzolana on the rheological, mechanical, and durability properties of self-compacting mortar. *Journal of Building Engineering*, 44. <https://doi.org/10.1016/j.jobe.2021.103276>
- Hassani, M. S.; J. C. Matos; Y. Zhang; and E. R. Teixeira** (2023). Green concrete with glass powder—A literature review. *Sustainability*, 15(20). <https://doi.org/10.3390/su152014864>
- Horsakulthai, V.** (2021). Effect of recycled concrete powder on strength, electrical resistivity, and water absorption of self-compacting mortars. *Case Studies in Construction Materials*, 15. <https://doi.org/10.1016/j.cscm.2021.e00725>
- Li, Q.; H. Qiao; A. Li; and G. Li** (2022). Performance of waste glass powder as a pozzolanic material in blended cement mortar. *Construction and Building Materials*, 324: 126531. <https://doi.org/10.1016/J.CONBUILDMAT.2022.126531>
- Li, X., and K. L. Scrivener** (2025). Quantification of nano-crystalline C-S-H in hydrated tricalcium silicate, Portland cement and fly ash cement using PONKCS method. *Cement and Concrete Research*, 191: 107837. <https://doi.org/10.1016/J.CEMCONRES.2025.107837>
- Lv, C., and J. Liu** (2023). Alkaline degradation of plant fiber reinforcements in geopolymer: A review. *Molecules*, 28(4): 1868. <https://doi.org/10.3390/MOLECULES28041868>
- Lyu, S.; J. Xiao; B. Wang; Y. Lu; and X. Sun** (2025). Influence of sisal fibers on mechanical properties and thermal conductivity of fully recycled aggregate concrete. *Construction and Building Materials*, 470: 140478. <https://doi.org/10.1016/J.CONBUILDMAT.2025.140478>
- Maraghechi, H.; M. Maraghechi; F. Rajabipour; and C. G. Pantano** (2014). Pozzolanic reactivity of recycled

glass powder at elevated temperatures: Reaction stoichiometry, reaction products and effect of alkali activation. *Cement and Concrete Composites*, 53. <https://doi.org/10.1016/j.cemconcomp.2014.06.015>

More, F. M. D. S., and S. S. Subramanian (2022). Impact of fibres on the mechanical and durable behaviour of fibre-reinforced concrete. *Buildings*, 12(9). <https://doi.org/10.3390/buildings12091436>

Nécira, B., and Y. Abadou (2021). Properties of self-compacting mortar made with various mineralogical sources different types of sands and fillers. *World Journal of Engineering*, 18(6): 861–869. <https://doi.org/10.1108/WJE-10-2020-0483>

Olofinnade, O. M.; J. M. Ndambuki; A. N. Ede; and C. Booth (2017). Application of waste glass powder as a partial cement substitute towards more sustainable concrete production. *International Journal of Engineering Research in Africa*, 31. <https://doi.org/10.4028/www.scientific.net/JERA.31.77>

Qu, W.; B. Niu; C. Lv; and J. Liu (2024). A review of sisal fiber-reinforced geopolymers: Preparation, microstructure, and mechanical properties. *Molecules*, 29(10): 2401. <https://doi.org/10.3390/MOLECULES29102401>

Rafi, A. Al; M. S. Ali; M. A. M. Hossain; and R. A. Redoy (2025). Experimental investigation on mechanical and physical properties of sisal fiber reinforced hybrid composites with filler material. *Next Research*, 2(3): 100509. <https://doi.org/10.1016/J.NEXRES.2025.100509>

Ren, Y.; Z. Yang; R. Kurihara; A. Tomoyose; and I. Maruyama (2025). Quantifying volcanic glass powder in cementitious systems using PONKCS-Rietveld analysis. *Materials and Structures*, 58(8): 273. <https://doi.org/10.1617/S11527-025-02796-6/TABLES/5>

Rodier, L., and H. Savastano (2018). Use of glass powder residue for the elaboration of eco-efficient cementitious materials. *Journal of Cleaner Production*, 184. <https://doi.org/10.1016/j.jclepro.2018.02.269>

Sales, R. B. C.; F. A. Sales; E. C. S. Corrêa; P. S. De Oliveira Patricio; N. D. S. Mohallem; and M. T. P. Aguilar (2015). Study of the influence of chemical composition on the pozzolanicity of soda-lime glass microparticles. *Materials Research*, 18. <https://doi.org/10.1590/1516-1439.343914>

Sara, B.; A. Mhamed; B. Otmane; and E. Karim (2023). Elaboration of a self-compacting mortar based on concrete demolition waste incorporating blast furnace slag. *Construction and Building Materials*, 366. <https://doi.org/10.1016/j.conbuildmat.2022.130165>

Wei, J., and C. Meyer (2015). Degradation mechanisms of natural fiber in the matrix of cement composites. *Cement and Concrete Research*, 73: 1–16. <https://doi.org/10.1016/J.CEMCONRES.2015.02.019>

Yimer, T., and A. Gebre (2023). Effect of fiber treatments on the mechanical properties of sisal fiber-reinforced concrete composites. *Advances in Civil Engineering*, 2023(1): 2293857. <https://doi.org/10.1155/2023/2293857>

Zhou, C.; F. Dai; Y. Liu; M. Wei; and W. Gai (2024). Experimental assessment on the dynamic mechanical characteristics and cracking mechanism of hybrid basalt-sisal fiber reinforced concrete. *Journal of Building Engineering*, 88: 109151. <https://doi.org/10.1016/J.JOBE.2024.109151>

Zhou, C.; M. Li; Q. D. Nguyen; X. Lin; A. Castel; Y. Pang; Z. Deng; T. Shi; and C. Mai (2025). Application of waste glass powder for sustainable concrete: Design, performance, perspective. *Materials*, 18(4): 734. <https://doi.org/10.3390/MA18040734>